Composition, Structure, Dynamics, and Evolution of Saturn's Rings

Article *in* Annual Review of Earth and Planetary Sciences · April 2010

DOI: 10.1146/annurev-earth-040809-152339

1 author:

Larry Esposito
University of Colorado Boulder
438 PUBLICATIONS **9,051** CITATIONS

Composition, Structure, Dynamics, and Evolution of Saturn's Rings

Larry W. Esposito

Laboratory for Atmospheric and Space Physics, University of Colorado, Boulder, Colorado 80309-0392; email: larry.esposito@lasp.colorado.edu

Annu. Rev. Earth Planet. Sci. 2010. 38:383–410

First published online as a Review in Advance on February 18, 2010

The *Annual Review of Earth and Planetary Sciences* is online at earth.annualreviews.org

This article's doi:
10.1146/annurev-earth-040809-152339

0084-6597/10/0530-0383$20.00

Key Words

giant planets, Saturn, planetary rings, disk dynamics, proto-planetary disks

Abstract

Cassini observations confirm that Saturn's rings are predominantly water ice. The particles in Saturn's rings cover a range of sizes, from dust to small moons. Occultation results show the particles form temporary elongated aggregates tens of meters across. Some of the ring structure is created by moons, others by various instabilities. Data from future Cassini measurements can help investigators decide if the rings are remnants of the Saturn nebula or fragments of a destroyed moon or comet.

1. INTRODUCTION

One of the most enduring symbols of space exploration is a planet surrounded by a ring. It is a wonderful surprise that the ringed planets are just as beautiful and scientifically compelling when seen close up! Furthermore, planetary rings are not just objects of beauty, but dynamic physical systems that provide an analogy for other flattened cosmic systems such as galaxies and planet-forming disks. We may even discover rings surrounding extrasolar planets.

Saturn's rings are the largest and brightest of the four ring systems surrounding each of the giant planets (for comparison, see Esposito 2006). They contain at least as much mass as Saturn's moon Mimas and display all the phenomena found in the other three smaller ring systems. This includes gaps with embedded moons and ringlets, narrow rings, broad rings, ethereal rings, waves, wakes, and wiggles. Ring D lies inside the brighter A, B, and C rings; ring E is a broad, tenuous ring centered on the moon Enceladus. The F ring is a narrow ring just outside the A ring, discovered by Pioneer 11 flyby in 1979, and the G ring is another narrow ring outside ring F: Cassini entered the Saturn system in an empty area between the F and G rings in July 2004.

Two views of Saturn's rings are shown in **Figures 1** and **2**: a Cassini image of sunlit Saturn and its rings (**Figure 1**) and the backlit planet and its rings from a vantage point of the planet's shadow (**Figure 2**). These images raise questions of the nature of Saturn's ring system: What are they made of? What causes the fine structure? What are the origin and history of these bright and massive rings? With the results of the Cassini-Huygens mission, which has orbited Saturn since 2004, we can now provide more detailed, albeit incomplete, answers to these questions.

Saturn's rings are dynamic and continually evolving. The rings change on timescales ranging from days to 10–100 million years, and each advance in observation reveals new structure! The ring particles are mainly aggregates of smaller particles arranged into transient elongated clumps tens of meters in size. Small moons near and within the rings are intimately involved in creating ring structure. Density waves excited by resonances with moons make up the majority of features in the A ring. Embedded moons create satellite wakes and perturb the edges of gaps cleared by these small moons. Propeller-shaped structures are an intermediate stage in which the embedded object is not large enough to hold open a complete gap.

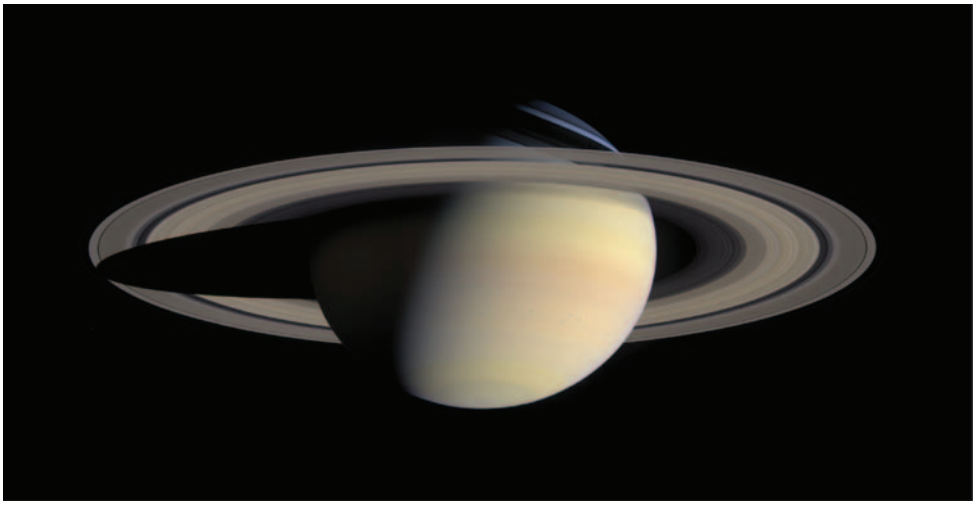

Figure 1

Saturn and its rings from the Cassini cameras. Image courtesy of NASA/JPL/Space Science Institute.

Figure 2

Saturn and rings in eclipse. Note the backlit rings, especially the diffuse E ring. Image courtesy of NASA/JPL /Space Science Institute.

The ring composition evolves with time: Photons, charged particles, and interplanetary meteoroids strike the rings. The rings may chemically evolve under the influence of oxygen in the ring environment. The ring system is not a homogeneous slab but is instead a two-phase system of gaps and dense clumps. Ring particles are primarily water ice, quite pure and dominantly crystalline. The reddish color of the rings shows a nonicy component, which may perhaps contain dark organics called tholins, polycyclic aromatic hydrocarbons, or nanohematite. The C ring and the Cassini Division are the most contaminated of the ring regions. The ring composition thus shows both primordial and extrinsic contributions. The lack of silicates indicates a parent body lacking a core or sequestration of the core material that keeps it from becoming mixed into the rubble of the rings.

Dynamical studies allow us to understand the underlying physical processes that create the myriad structures. The self-gravity of the particles is important, and the particles continually form temporary gravitationally bound clumps. These self-gravity wakes show the equilibrium established between the gravitational attraction of the particles and the Kepler shear of their orbits around Saturn. Dense packing leads to strong nonlocal contributions to the pressure and momentum transport. This gives rise to viscous overstability, yielding axisymmetric waves of 100-m wavelength. Both accretion and fragmentation are important in the evolution of the ring system. Saturn's F ring is itself a showcase of accretion.

The question of the origin and evolution of the ring system is still unsolved. Three proposed models are that the rings are (*a*) remnants of the Saturn nebula, (*b*) the debris from a destroyed satellite, or (*c*) the remnants of a split comet. The rings could be ancient if they are continually renewed. A solution to the puzzle of ring origin is therefore the possibility of recycling primordial material. In this case, the rings are likely much more massive than suggested by analysis of Voyager data, which indicated that the rings contain as much mass as Saturn's small moon Mimas. Furthermore, the youngest ring features might have been recreated a number of times. If the rings were created by the destruction of a small moon during the period of the Late Heavy Bombardment (the cataclysm that also created the great lunar basins), recycling would still be necessary for the rings to survive to the present time. Saturn's E ring is created by geologic activity on Enceladus.

Self-gravity wakes: temporary, elongated gravitational aggregations that form in a sheared medium within the Roche zone

Kepler shear: in accordance with Kepler's law, the angular velocity of orbiting material declines with distance, creating a shear in the disk

Overstability: an instability of shear flow that creates axisymmetric waves

The G ring is fed by moonlets embedded within it. Diffuse rings are associated with tiny moons (Janus, Epimetheus, Pallene, Methone, and Anthe), reminiscent of Jupiter's ring.

This article benefits from previous reviews by Cuzzi et al. (1984. 2004), Esposito et al. (1984), and Esposito (1993, 2002, 2006). For the interested reader, many more details can be found in selected chapters of the recent book *Saturn from Cassini-Huygens* edited by Dougherty et al. (2009) (Charnoz et al. 2009a, Colwell et al. 2009b, Cuzzi et al. 2009, Horanyi et al. 2009, Schmidt et al. 2009).

2. RING COMPOSITION AND STRUCTURE

Saturn's rings are composed of a myriad of individual particles that continually collide. The ring particles are actually agglomerates of smaller elements that are at least temporarily cohering: These temporary bodies are subject to both growth and fragmentation. The balance between the competing processes yields a distribution in size and velocity that varies in time owing to stochastic events.

2.1. Ring Particle Size and Shapes

The size of Saturn's ring particles extends over many decades, from fine dust to embedded moonlets, kilometers across. The observations can often be fit with a power law

$$N(a)da = C_0 a^{-q}\, da \quad \text{for} \quad a_{min} < a < a_{max}, \tag{1}$$

where C_0 is a constant, and a_{min} and a_{max} are the radii of the smallest and largest particles in the distribution. Typical values of q are approximately 3, which is also characteristic of the asteroid belt and of size distributions created by shattering objects in the laboratory. This similarity is likely not coincidental: Both the asteroids and particles in planetary rings were probably created by fragmentation of larger objects and were subjected to subsequent collisional evolution. For $q < 4$, most of the mass is in the larger particles. In most of the rings, a_{min} is the range 1–30 cm and a_{max} is 2–20 m.

Numerical simulations show how the collisions between particles redistribute the energy of their random motion. In ideal gases, the state of thermal equilibrium leads to equipartition of energy between particles of different sizes. For rings, owing to the dissipative nature of the collisions, this state is only partly reached: The smaller bodies have only 2% to 20% of the kinetic energy of the largest ring particles (Salo 2001). However, because of their much smaller masses, the small ring particles still have significantly higher velocities relative to a purely circular orbit. These larger velocities represent larger eccentricities and inclinations that cause the vertical excursions of small particles to be larger. Thus, the particle size distribution leads to a vertical gradient in particle size: The largest particles, with most of the mass of the ring system, are confined to nearly a monolayer in the ring plane, whereas the smaller particles extend to higher altitudes.

2.2. Rubble Piles

The collisions of the ring particles can cause them either to grow in size or to be disrupted. The dynamic balance between these competing processes establishes an equilibrium state of aggregate bodies that resemble piles of rubble [called dynamic ephemeral bodies by Weidenschilling et al. (1984)]. Particles tend to gather together, quickly growing to sizes that resist tidal disruption, only to be broken apart by mutual collisions. Because relative velocities are low and collisions are inelastic, accretion is rapid. Large particles can hold smaller ones on their surfaces by their

mutual gravitational attraction (Canup & Esposito 1995) or by adhesion (Albers & Spahn 2006). In Saturn's rings, the timescale is only weeks for house-sized objects to accrete. These large rubble piles are indeed dynamic and ephemeral: Such rubble piles are a complete contrast to the idealized model that the rings consist of spherical ring particles of a uniform size. The temporary aggregations are typically elongated and sheared, as seen in numerical simulations (e.g., Lewis & Stewart 2005), self-gravity wakes (Colwell et al. 2007), and one partially transparent F-ring feature, Pywacket, observed by Cassini UVIS and VIMS (Esposito et al. 2008b).

2.3. Ring Particle Composition

In general, particles in planetary rings are similar to the nearby moons. Saturn's rings are predominantly water ice, Uranus's are dark, and Jupiter's are derived from nearby Thebe and Amalthea. Although Saturn's rings are dominantly crystalline water ice, they are visually red, showing some contamination by nonicy material (e.g., Cuzzi et al. 2009).

Color variations across Saturn's rings (Cuzzi et al. 2009) may indicate varying composition, including effects of the interplanetary dust that bombards them and darkens the particles. Saturn's ring particles have rough, irregular surfaces resembling frost more than solid ice. There is good indication that the particles are less dense than solid ice, supporting the idea of ring particles as temporary rubble piles. These slowly spinning particles collide gently with collision velocities of usually just millimeters per second.

A recent suggestion is that the red color of the rings results from iron oxidized to hematite (R. Clark et al., manuscript submitted). Nanohematite (very fine-grained hematite Fe_2O_3) is a strong UV absorber that matches the ring spectrum (**Figure 3**). The oxidation may be the result of chemical reactions with the ring atmosphere (which contains the water products H_2O, OH, O, H, H_2, and O_2 and their ions) (Johnson et al. 2006). The atmosphere over the rings is dominated by molecular oxygen (O_2). There is no spectral evidence for silicates in the ring particles (R. Clark et al., manuscript submitted).

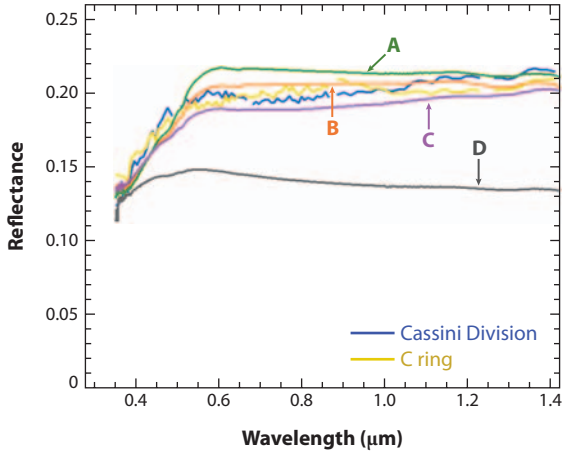

Figure 3

Spectra of laboratory analogs compared with Cassini VIMS spectra of Saturn's rings. Laboratory spectra at temperatures 84–90 K of ice mixtures with nanohematite and other possible absorbers (A, B, C and D) are shown. Figure taken from R. Clark et al. (manuscript submitted).

2.4. Ring Structure

Our understanding of the structure of Saturn's rings has improved dramatically over the course of the Cassini mission, in large part because of the combination of observations from multiple instruments taken from a wide range of geometries. This has enabled, for the first time, a detailed exploration of nonaxisymmetric structures in the rings as well as the vertical structure of the main rings. The macroscopic structure of Saturn's rings is nearly identical to that which was observed by Voyager. The most notable exception is the change in morphology of the F ring, which has continued to evolve underneath Cassini's multiwavelength eyes.

The grand structure of the rings is shown in **Figure 4**, a composite of stellar occultation measurements and a Cassini imaging mosaic. Saturn's rings can be grouped into the classical dense rings (A, B, and C) and tenuous rings (D, E, and G). The Cassini Division separating the brightest rings A and B is not empty and resembles the C ring. Ring F shares some characteristics of both dense and diffuse rings, along with a population of embedded objects.

The most common structures in the rings are density waves excited by the gravity of nearby moons, at locations where the ring particle motion is resonant with the moon. **Figure 5** shows the A ring and the outer Cassini Division. Each wave is labeled by the ratio of the particle mean motion to that of the moon. For the Mimas 5:3 resonance, both the density wave and bending wave are evident. Bending waves are a corrugation of the ring caused by resonance with an inclined moon. A close-up Voyager image of these two types of waves is shown in **Figure 6**.

In addition to density and bending waves, nearby moons can also create wakes and wavy edges in the rings. **Figure 7** shows the variety of features in a region around Saturn's Encke Gap in the outer A ring. Pan is the moon whose gravity clears the gap (Showalter 1991), not visible in this

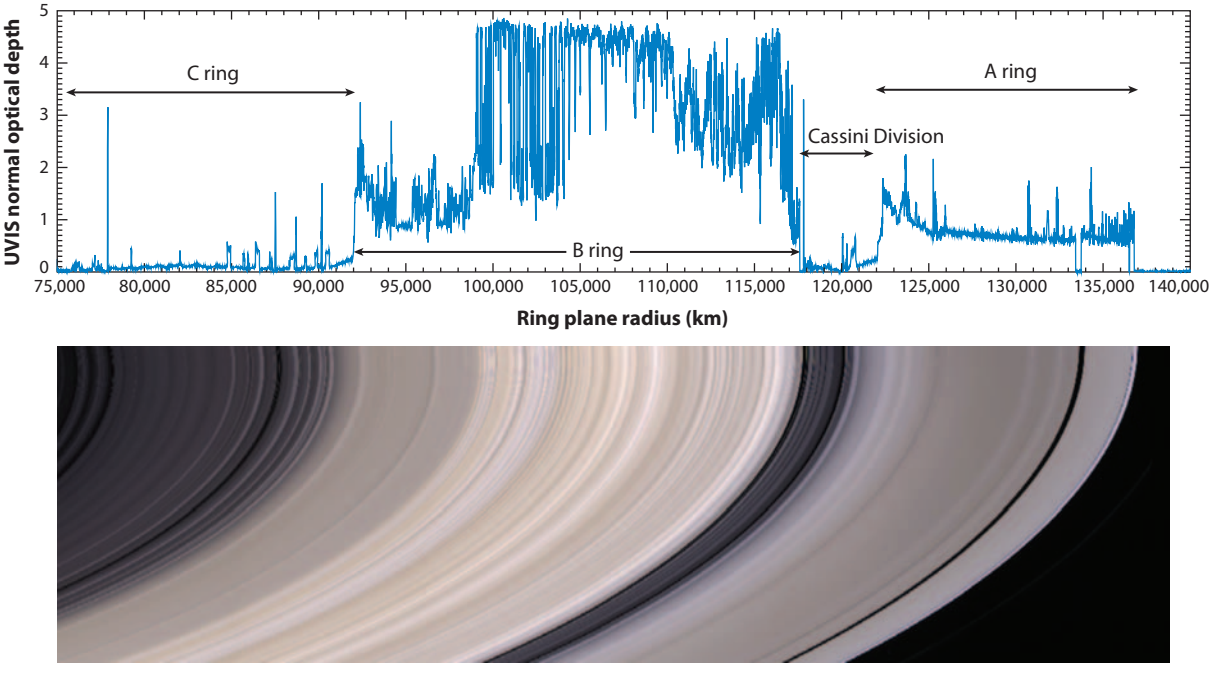

Figure 4

ISS mosaic and UVIS stellar occultations measurements showing structure in Saturn's rings. Resolution is 10 km. Reprinted from figure 13.1, Colwell et al. 2009b, with kind permission from Springer Science and Business Media.

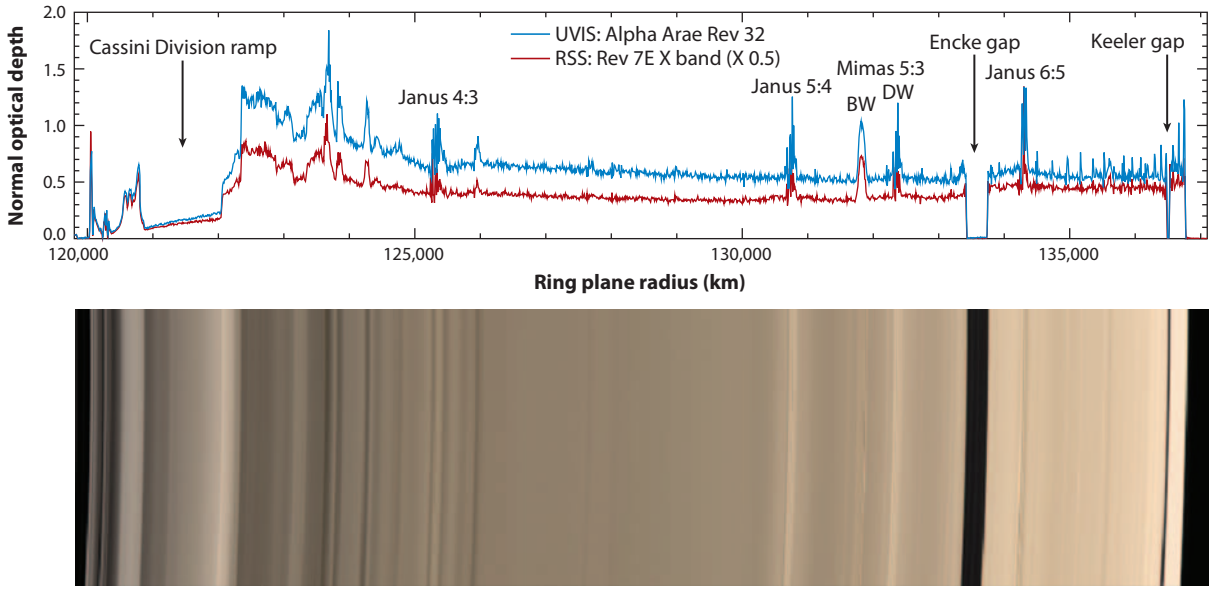

Figure 5

The A ring and outer Cassini Division from Cassini UVIS and RSS occultation profiles, compared with an ISS mosaic. Resolution is 6 km (image) and 10 km (occultations). BW, bending wave; DW, density wave. Reprinted from figure 13.2, Colwell et al. 2009b, with kind permission from Springer Science and Business Media.

particular image (for more details, see Colwell et al. 2009b, Horanyi et al. 2009, Schmidt et al. 2009).

Density waves provide a local probe of the ring properties: The wave dispersion gives the surface mass density, and the attenuation of the wave amplitude gives the viscosity, which can be related to the interparticle collision velocity and the ring thickness (see, e.g., Tiscareno et al. 2007,

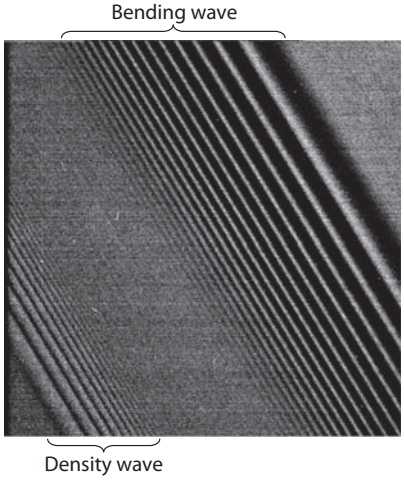

Figure 6

Voyager image of density wave and bending wave. Image courtesy of NASA/JPL.

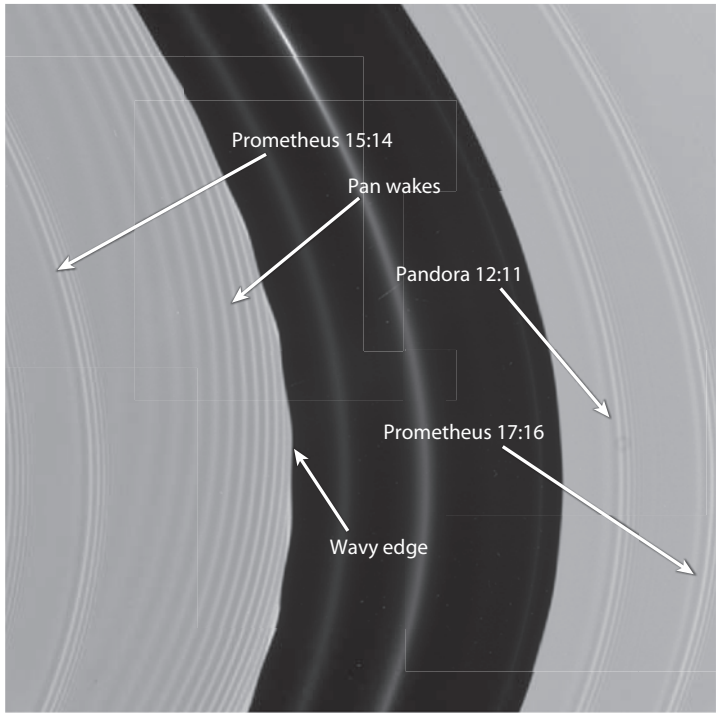

Figure 7

The Encke Gap (320-km width) imaged by Cassini at Saturn Orbit Insertion. Note the dusty ringlets within the ring, a wavy inner edge recently perturbed by the satellite Pan (not within the image) and satellite wakes. Density waves are labeled by the resonance that launches them. Reprinted from figure 13.4, Colwell et al. 2009b, with kind permission from Springer Science and Business Media.

Colwell et al. 2009a). **Figure 8** shows that the waves in the outer part of Saturn's rings indicate a density of 1–60g cm^{-2} and a velocity of 0.3–10 mm s^{-1}, implying a thickness of 3–5 m in the Cassini Division and 10–15m in the inner A ring.

A major Cassini finding was the discovery and characterization of self-gravity wakes (Colwell et al. 2006, 2007; Hedman et al. 2007b) from the comparison of multiple star occultations. The first Cassini occultations gave variable values for the transparency of the ring! This longitudinal variation can be explained by the fact that the ring is not uniform but is instead clumped into temporary aggregations. Because the aggregations are sheared by the outward decrease in Kepler orbital velocity, they have a preferred elongation tilted 20–25° to the local orbital flow; this explains how the viewing angle yields different optical depth (**Figure 9**). No massive seed particle is required to form the wakes: Unlike satellite wakes, they are not wakes in the usual sense of the word (Colwell et al. 2006).

Azimuthal brightness asymmetry: longitudinal variation of Saturn's A-ring brightness with two maxima and minima, also seen in the B ring

The A-ring optical depth variations are most pronounced in the central A ring, which is also the location of the peak amplitude of the azimuthal brightness asymmetry. This asymmetry (Camichel 1958, Lumme et al. 1983) provided the first clue to the existence of these self-gravity wakes. Simulations by Salo (1992, 1995) demonstrated that such wakes arise naturally in a self-gravitating ring. Porco et al. (2008) and French et al. (2007) included the wakes to reproduce Voyager, Cassini, and Hubble observations of the A-ring brightness asymmetry. Their numerical results indicate that ring particle collisions must be dissipative.

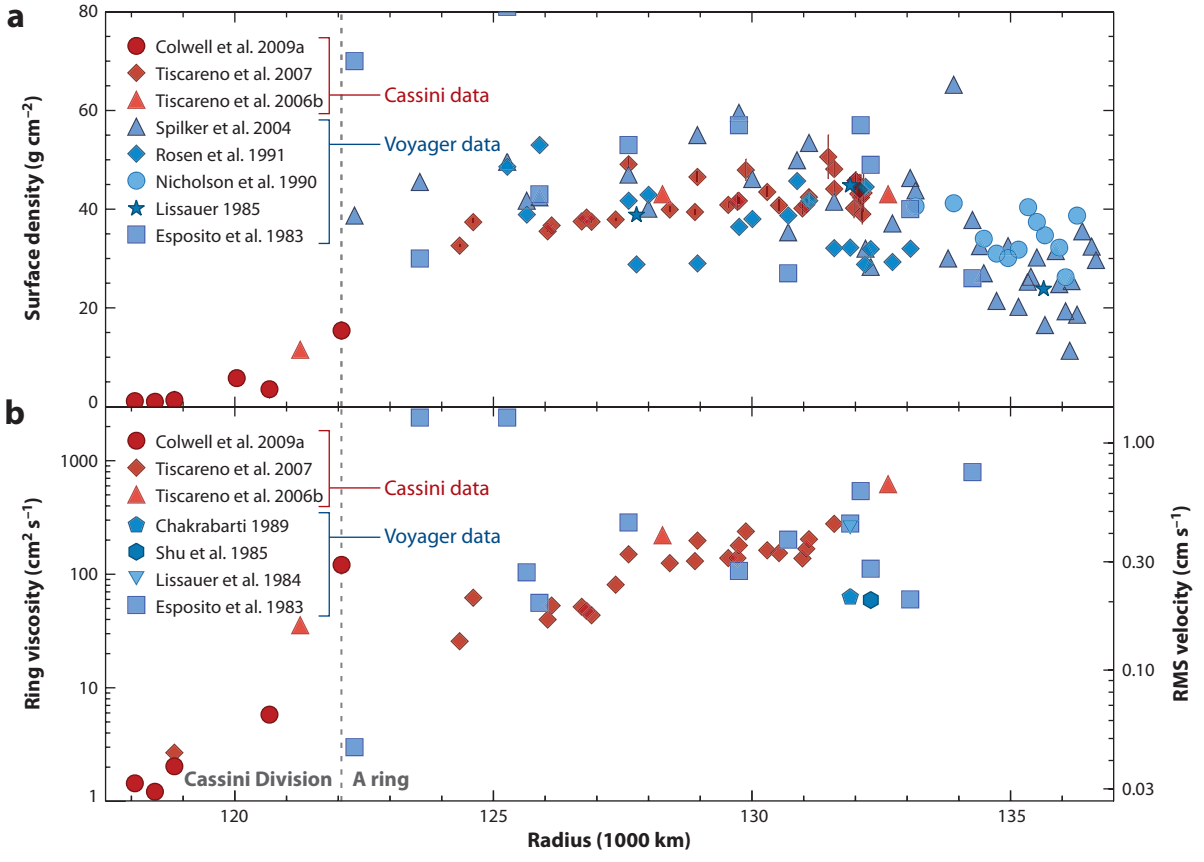

Figure 8

Surface density (*a*) and viscosity (*b*) of Saturn's A ring and Cassini Division, from analysis of density waves. Bottom right-hand scale is the inferred random velocity. Reprinted from figure 13.3, Colwell et al. 2009b, with kind permission from Springer Science and Business Media.

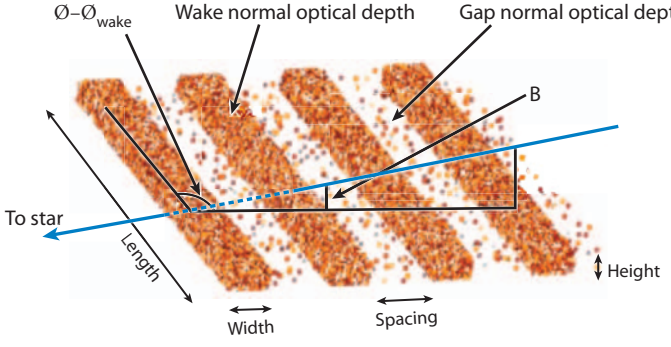

Figure 9

The so-called granola-bar self-gravity-wake model. Model parameters affecting measured optical depth are indicated. The blue line is the line of sight to occulted star. The wake orientation is given by $\phi - \phi_{wake}$. The star declination is B. For more details, see Colwell et al. (2006).

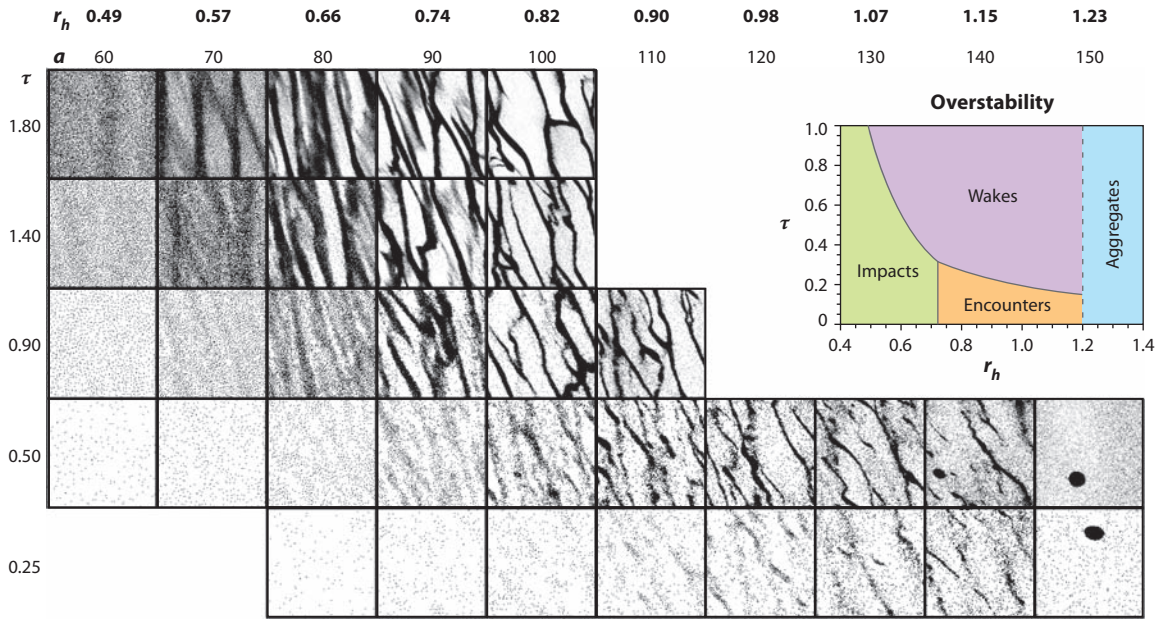

Figure 10

Simulations of ring structure for values of optical depth (τ) and distance from Saturn (a) in units of 10^3 km. The relative strength of self-gravity to tidal force is given the parameter r_h (ratio of Hill radius to particle radii) for particle mass density 0.9 g cm^{-3}. (*Upper left*) Axisymmetric overstable occultations coexist with inclined self-gravity wakes. (*Inset*) Summary of the locations at which processes dominate. Reprinted from figure 14.7, Schmidt et al. 2009, with kind permission from Springer Science and Business Media.

Detailed models of the Cassini occultations (Colwell et al. 2006) and thermal emission (Leyrat et al. 2008) show the wakes are highly flattened, with a height-to-width ratio of 0.2 to 0.4. Between the wakes are nearly transparent gaps with optical depth 0.1 to 0.3. These findings mean that previous interpretations have significantly underestimated the amount of material in the rings. Because of the self-gravity wakes, the average transmission is determined primarily by the width and transparency of the narrow gaps between the wakes (Colwell et al. 2007), rather than the total cross section of particles. For practical purposes, the gaps are almost empty. Numerical simulations that incorporate a range of particle sizes (e.g., Salo & Karjalainen 2003) predict that the larger particles are concentrated in the wakes, with smaller centimeter-sized particles distributed more evenly. This prediction leads to a picture of Saturn's B ring in which broad, flat wakes of densely packed meter-size particles lie in a thicker, low-density haze of small particles. The measured optical depth may further underestimate the amount of ring material because it does not reflect particles hidden within the opaque B-ring wakes (Stewart et al. 2007, Robbins et al. 2009).

Figure 10 displays a simulation survey of wake structures expected at different planetocentric distances. The figure indicates clearly the gradual increase in the strength of wakes as the assumed distance or optical depth increases, as well as the increase in the clumpiness of the wakes, and their eventual collapse into aggregates at large distances.

We know that moons embedded in the rings can open gaps, as Pan creates the Encke Gap and Daphnis creates the Keeler Gap. It was expected that small moons would explain the multiple gaps in the C ring and the Cassini Division. However, to date, no moons have been found.

Instead of finding these suspected moonlets in empty gaps, Cassini indirectly discovered evidence for moonlets that only partially open gaps. If an embedded moonlet is smaller than a few

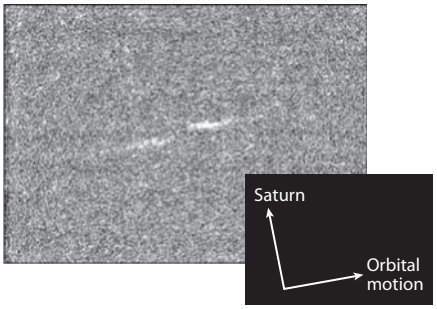

Figure 11

Propeller feature observed by Cassini on July 1, 2004. Image courtesy of NASA/JPL/Space Science Institute.

hundred meters, then the gap it induces in the rings may be closed by viscous diffusion before it extends completely around the ring. The competition between gravitational scattering and viscous diffusion creates a typical structure shaped like the letter S, which has been termed a propeller (Spahn & Sremcevic 2000). Such S-shaped density undulations, induced in a disk as the local response to an embedded mass, were first studied by Julian & Toomre (1966).

Propeller objects: unseen objects that create S-shaped structures in Saturn's rings

The first four propeller features (**Figure 11**) were seen in Cassini images by Tiscareno et al. (2006a). A large number of propellers were found preferentially interior to the Encke Gap (Sremcevic et al. 2007, Tiscareno et al. 2008). The exact interpretation of the propeller features is still disputed: Do the brighter regions seen in the images indicate more or less material? Photometric modeling by Sremcevic et al. (2007) interpreted the bright regions as wakes of enhanced density where the brightness is increased by release of regolith from colliding particles (**Figure 12**).

These propeller-creating objects show a very steep size distribution, with power-law index of $q = 6$ (Tiscareno et al. 2008, from the largest data set). They therefore appear to be a distinct

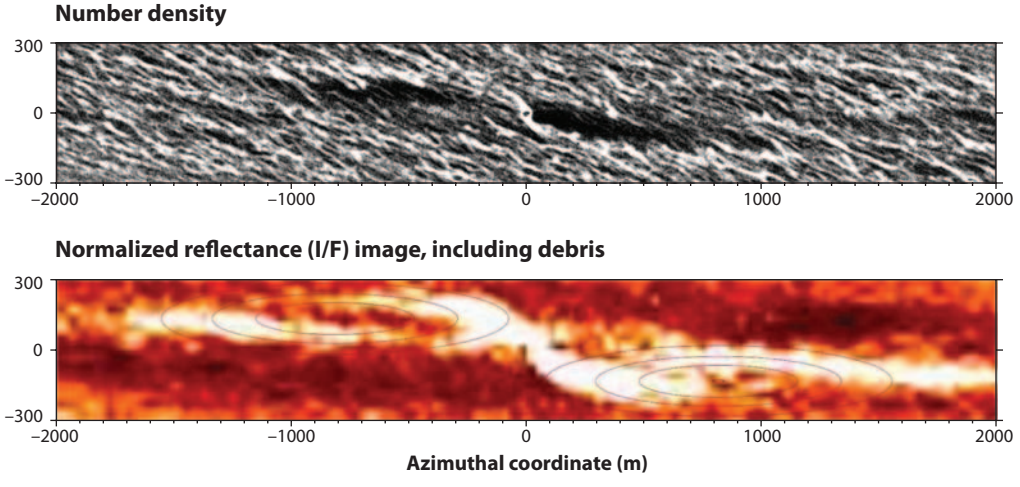

Figure 12

Numerical models of propellers. (*Upper panel*) Particle density distribution perturbed by 40-m-diameter moonlet. (*Lower panel*) Synthetic image for comparison with **Figure 11**, including loosely bound regolith. The released debris hides the predicted gaps in the numerical model and enhances the brightness of the density crests. Reprinted from figure 14.16, Schmidt et al. 2009, with kind permission from Springer Science and Business Media.

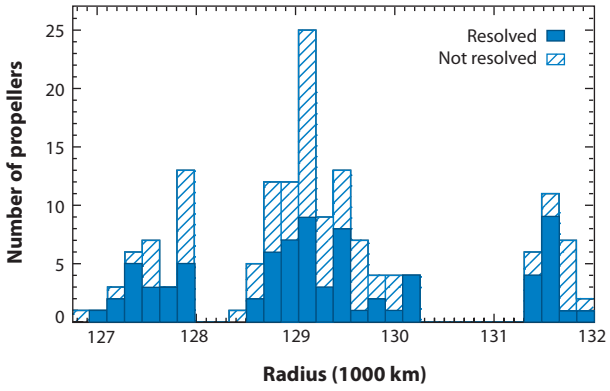

Figure 13

Radial distribution of 100-m diameter propellers. Three distinct belts are seen. Figure modified from Tiscareno et al. (2008), reproduced by permission of the AAS.

distribution from the majority of ring particles. Furthermore, the moons Pan and Daphis (which open the Encke and Keeler gaps) do not fit on this distribution. Schmidt et al. (2009) suggested three families of bodies in the rings: ring particles (1 cm < a < 10 m; see Equation 1), propeller moonlets (10 m < a < 500 m), and ring moons (0.5 km < a < 100 km), consistent with the scenario of ring formation in episodic cascades where ring moons and moonlets are continuously destroyed by meteroid impacts (Esposito et al. 2005; see below). The steep moonlet size distribution may be essential; otherwise, frequent interactions with neighboring larger moonlets would destroy the propeller feature (Lewis & Stewart 2009).

The propellers are concentrated into three bands of roughly 1000-km width (Tiscareno et al. 2008; see **Figure 13**) at the same distance from Saturn where the azimuthal brightness asymmetry is maximum and where the self-gravity wakes are strongest. Are the wakes created by fragments of an earlier destroyed object, or is this a region of increased accretion where aggregates have grown to sizes that are capable of creating propeller structures?

Exterior to the Encke Gap, only a few (generally larger) propellers are seen. The largest propellers clearly show the theoretically expected incomplete gaps and the moonlet-induced wakes. Fluctuations in the ring surface mass density may cause a stochastic migration of the moonlet (Burns et al. 2008), as seen in simulations (Lewis & Stewart 2009). A similar effect (type III migration) has been suggested for growing planetary embryos embedded in preplanetary gas-dust disks (Masset & Papaloizou 2003, Papaloizou et al. 2007).

2.5. Saturn's F Ring: Processes and Origin

Saturn's F ring is one of the most dynamic objects in the Solar System. It was discovered by the author as a member of the Pioneer 11 imaging experiment in 1979 (Gehrels et al. 1980). This narrow ring lies 3400 km beyond the A ring's outer edge, precisely at the classical Saturn's Roche limit for ice (see Section 3.1.1). In 1980, the ring appeared with much greater clarity under the scrutiny of the Voyager 1 cameras, which revealed a remarkable wealth of longitudinal structures, including clumps, kinks, and so-called braids (Smith et al. 1981, 1982). Twenty-five years later, Cassini has provided high-resolution occultations (Albers et al. 2010), images, maps, and movies of the F ring, confirming numerous transient structures (**Figure 14**). In addition to the ring, sharp drops in the flux of magnetospheric electrons detected by Pioneer 11

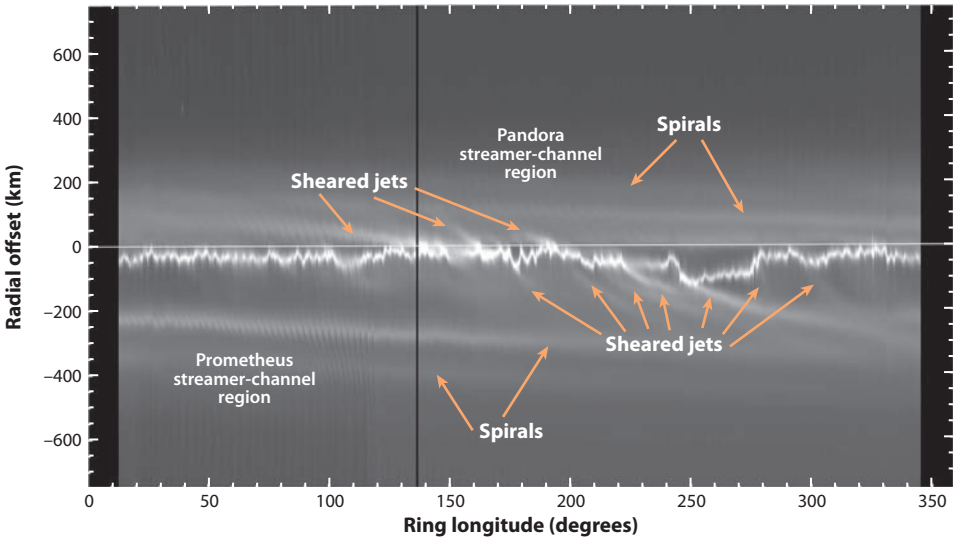

Figure 14

Mosaic of reprojected images of the F ring, annotated to show the prominent jets, spirals, and channels due to Prometheus and Pandora (see Murray et al. 2008). Reprinted from figure 13.24, Colwell et al. 2009b, with kind permission from Springer Science and Business Media.

suggested the presence of an underlying moonlet belt (Cuzzi & Burns 1988). This model is similar to the modern image of a circumstellar debris disk, such as that for Beta-Pictoris (see, e.g., Lagage & Pantin 1994), in which unseen small-bodies belts, stirred by planets, produce a dusty disk visible due to its infrared excess. Charnoz 2009 and Murray et al. 2008 proposed that the population of moonlets (see **Figure 15**) exterior to the core (among which the satellite designated S2004/S6 is a member) regularly collides with the population inside the core, releasing material whose orbital motion forms structures named spirals (Charnoz et al. 2005) or jets. Several moonlets that could be members of this putative belt have been discovered in Cassini images (Porco et al. 2005; Murray et al. 2005, 2008) and in stellar occultations (**Figure 16**). The F ring is also famous for its shepherding moonlets, Pandora and Prometheus, which were believed initially to confine the ringlet radially (Goldreich & Tremaine 1979) and are known to interact chaotically (French et al. 2003, Goldreich & Rappaport 2003). However, the present understanding is much more complex, and it is not clear if this mechanism is really responsible for the F ring's narrowness. Lewis and colleagues (Lewis & Stewart 2005; M.C. Lewis, G.R. Stewart, J. Leezer, and A. West, private communication) propose a collisional process to create this narrow ring.

Very-high-resolution images of the F-ring core (Murray et al. 2008) reveal a wealth of kilometer-scale dynamical structures in the core that still remain to be explained. Conversely, the envelope and strands that surround the core are made of micrometer-sized dust, shining at high phase angles with a steep particle size distribution ($q \sim 4.6$) (Showalter et al. 1992). Showalter (1998, 2004) proposed that transient bright features are dust clouds generated by meteoroid bombardment, whereas other authors suggested that the local collisional activity implying moonlets (or clumps) could be the cause of these events (Poulet et al. 2000, Barbara & Esposito 2002, Charnoz 2009). Recent Cassini image data seem to support the latter model (Charnoz et al. 2005, Charnoz 2009, Murray et al. 2008).

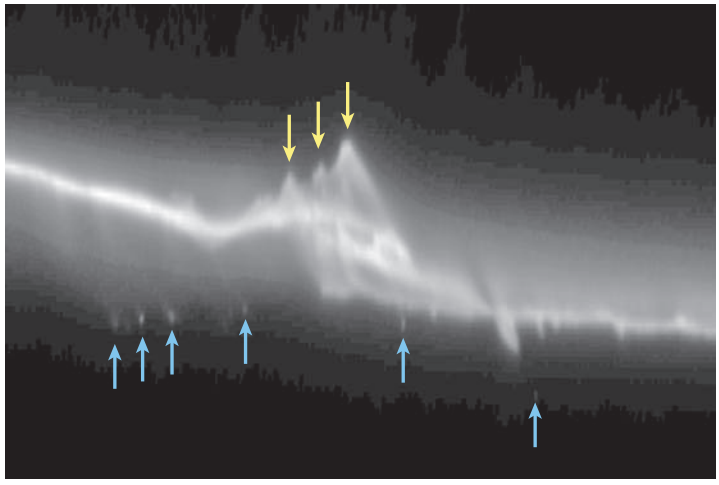

Figure 15

Reprojected Cassini image indicating evidence for small ($\lesssim$1-km) objects (*blue arrows*) in the F ring, along with possible corresponding features they create (*yellow arrows*). Reprinted from figure 13.26, Colwell et al. 2009b, with kind permission from Springer Science and Business Media.

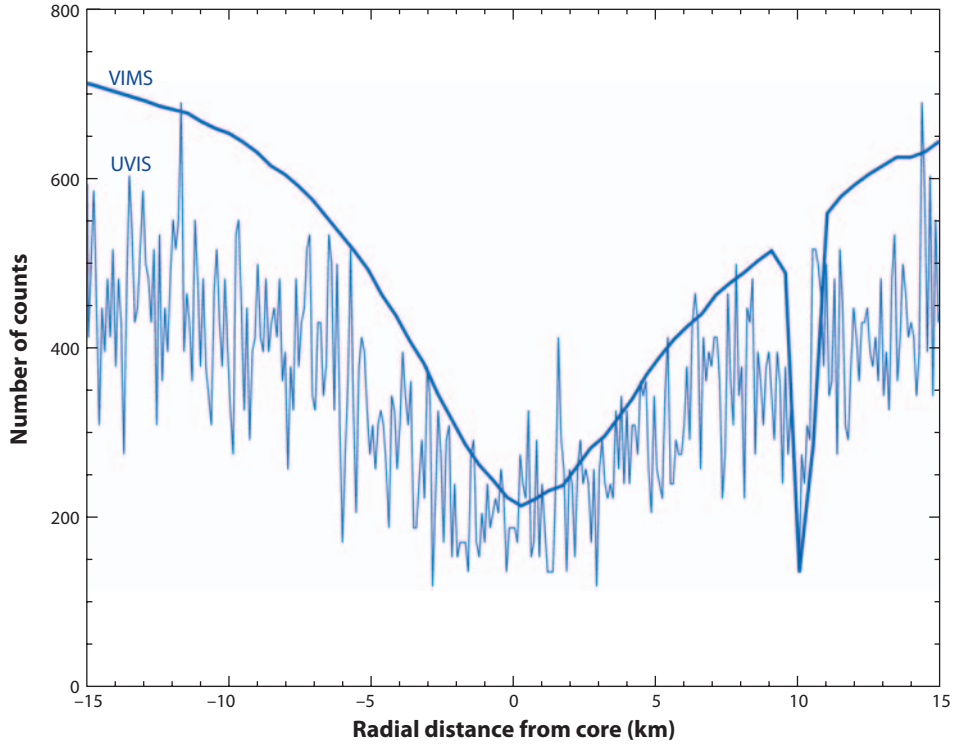

Figure 16

Simultaneous VIMS (*solid*, *smooth curve*) and UVIS (*thin curve*) occultation profiles showing the feature Pywacket approximately 10 km outside the F-ring core. Figure taken from Esposito et al. (2008b).

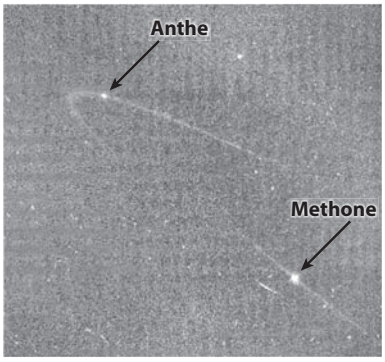

Figure 17

Image of debris arcs associated with small moons Anthe and Methone. Figure taken from Hedman et al. (2009). Image courtesy of NASA/JPL/Space Science Institute.

It seems that the F-ring origin is linked to the origin of a population of parent kilometer-sized moonlets. Cuzzi & Burns (1988) proposed that a small moon was destroyed in the past, whose fragments are slowly eroding today. Conversely, Barbara & Esposito (2002) suggested that there is ongoing accretion in the F-ring core, producing clumps and moonlets, whose subsequent collisional erosion produces the F ring.

2.6. Diffuse Rings

Diffuse planetary rings are an excellent laboratory to study dusty plasma processes. The dust grains are mostly collisional debris from small moons that resupply the ring through collisions and meteoritic impacts on their surfaces. In the Saturn system, diffuse rings are associated with tiny moons (Janus, Epimetheus, Pallene, Methone, and Anthe) (see **Figure 17**). The broad E ring (**Figure 18**) is created by eruptions on the moon Enceladus (see Kempf et al. 2009). A population of source bodies has been found in the G ring (Hedman et al. 2007a). These dusty rings are influenced by solar and radiation forces and are sculpted by periodic forces. For many details, the reader is referred to the recent review by Horanyi et al. (2009).

3. DYNAMICS AND EVOLUTIONARY PROCESSES

3.1. Basic Concepts and Timescales

Saturn's rings are an ensemble of numerous particles, subject to Saturn's gravity, subject to gravity and collisions from other particles, bombarded by meteorites, and subject to various instabilities. Some simple relationships allow us to estimate timescales and stability.

3.1.1. Roche zone. Roche (1847, see Chandrasekhar 1969) calculated the distance at which a purely fluid satellite would be pulled apart by tidal forces. Inside this distance, a fluid satellite cannot attain hydrostatic equilibrium. Of course, solid objects (and humans, for example) can exist inside the Roche limit without being disrupted by tides due to their material strength. Even loose aggregates would possess some strength.

Roche zone: the region around the Roche limit where accretion competes with the tidal forces from the planet

Roche's criterion can be written as

$$\frac{\alpha_r}{R} = 2.456 \left(\frac{\rho_p}{\rho}\right)^{1/3}, \qquad (2)$$

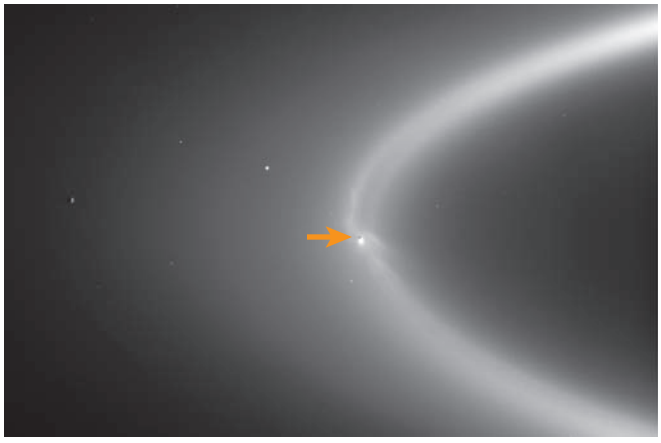

Figure 18

Enceladus (*small black dot indicated by arrow*) eruptions feeding Saturn's E ring. Image courtesy of NASA/JPL/Space Sciences Institute.

where fluid objects would suffer tidal disruption inside the Roche limit, α_r, for a central planet with radius R and density ρ_p, and the particle's density is ρ. Thus, more dense objects could avoid tidal disruption closer to the planet. For real bodies, stripping of loose material or fracture by tidal stresses occurs much closer to the planet than in Equation 2 (see Smoluchowski 1978, 1979).

Canup & Esposito (1995) studied accretion inside the classical Roche limit in the case in which one body is much larger than the other. In fact, if they are not rotating, a small body on the surface of a larger one is held by its gravitational attraction if

$$\frac{\alpha}{R} \geq 1.26 \left(\frac{\rho_p}{\rho}\right)^{1/3}. \tag{3}$$

The region surrounding the classical Roche limit, where the difference in tidal force for two bodies in contact is comparable in magnitude to their mutual gravitational attraction, is called the Roche zone. This is the same region where accretionary growth must compete with tidal disruption, so that the formation of natural satellites around the planet would also be impeded there.

3.1.2. Rapid flattening of an initial disk. A planetary ring consists of small particles in nearly circular orbits, with orbital speed given by Kepler's law,

$$\Omega = \sqrt{\frac{GM}{r^3}}, \tag{4}$$

where M is the central planet mass, G is the gravitational constant, r is the distance from the center, and Ω is the angular rotation rate. The optical depth of a ring of equal-sized particles is

$$\tau = \pi a^2 \Sigma / m, \tag{5}$$

where a and m are the radius and the mass of an individual particle, respectively, and Σ is the surface mass density of the disk. This yields the collision frequency of at least 2τ each orbit because a particle on even a slightly inclined orbit will cross the ring plane twice. More detailed calculations and the inclusion of self-gravity lead to even higher collision rates. For an optically thick ($\tau \geq 1$) ring, such as Saturn's B ring, collisions occur every few minutes.

This rapid collision rate explains why each ring is a nearly flat disk. Starting with a set of particle orbits on eccentric and mutually inclined orbits (e.g., the fragments of a small, shattered moon), collisions between particles dissipate energy but also must conserve the overall angular momentum of the ensemble. Thus, the relative velocity is damped out, and the disk flattens after only a few collisions to a set of nearly coplanar, circular orbits (Brahic 1976).

Ballistic transport: meteoroid impacts on Saturn's rings move material and alter its composition

After achieving this flattened state, the disk of the planetary ring evolves, but more slowly, dominated by the Kepler shear. The system continues to lose energy in collisions and to conserve momentum. In a collision between two particles on nearly circular orbits, the inner ring particle loses angular momentum and falls to a lower (and thus, by Kepler's laws, a faster) orbit, whereas the opposite is true of the outer particle. The result is that the two particles diverge. The overall evolution of the ring reflects this: It spreads! The net angular momentum transfer is outward, while the mass of the ring is gradually transferred inward. If there are no barriers to this inward diffusion, the ring particles will eventually reach the planet's atmosphere, each to burn up as a meteor. Lynden-Bell & Pringle (1974) found the same result for accretion disks around black holes.

3.1.3. Mean free path and timescales. Here we consider the mean free path λ (average radial distance between collisions). For optically thick rings, this is just the average random speed c multiplied by the time between collisions: $\lambda = c/(\Omega\tau)$, where Ω is orbital frequency. For very thin rings, the mean free path is given by $\lambda = c/\Omega$ as the time between collisions is more like the orbital period. Cook & Franklin (1964) included both limiting values in their prescription [which was also adopted by Goldreich & Tremaine (1978)]:

$$\lambda^2 = \frac{c^2}{\Omega^2}\frac{1}{1+\tau^2}. \quad (6)$$

The behavior of any individual particle experiencing repeated collisions can be seen as an aspect of a simple random walk with the step size in radius given by λ. We let $\Delta r = n\lambda$. For a random walk, it takes on the average n^2 steps to reach a distance $n\lambda$ from the origin. Thus, the time for a typical particle to diffuse a distance Δr is n^2 steps each of duration $\Delta t = 1/(\Omega\tau)$, giving the total time for a particle to diffuse a distance Δr

$$T \approx \frac{(\Delta r)^2}{\nu}, \quad (7)$$

where the viscosity ν can be derived from Equation 6. This simple expression does not hold for dense rings (e.g., Daisaka et al. 2001). The finite sizes and the gravity of the ring particles (due to enhanced transport by self-gravity wakes) are responsible for a global increase of the viscosity with optical depth that goes as $\nu(\tau) \propto \tau^\beta$ with $\beta \geq 2$ (Schmidt et al. 2009). As a consequence, the rings would spread more rapidly due to the presence of self-gravity wakes. For values typical of Saturn's A ring, $\nu = 100$ cm^2 sec^{-1} (Schmidt et al. 2009), ring-spreading times are less than a billion years.

3.1.4. Meteoritic bombardment and ballistic transport. Because the rings have a large surface area-to-mass ratio, they are particularly susceptible to modification due to extrinsic meteoroid bombardment. The vast majority of the dust and debris produced from these impacts is ejected at speeds much less than the velocity needed to escape the rings. As a result, a copious exchange of ejecta between different ring regions can occur, which over time can lead to the structural and compositional evolution of the rings on a global scale. This process by which the rings evolve subsequent to meteoroid bombardment is referred to as the ballistic transport of impact ejecta (Ip 1983; Durisen 1984a,b; Lissauer 1984).

Impact ejecta from a given meteorite impact are thrown predominantly in the prograde orbital direction. This result arises naturally from consideration of impact geometries and probabilities azimuthally averaged over the rings (Cuzzi & Durisen 1990). The yield of a single impact can be on the order of $\sim 10^5$–10^6 times the impactor mass. Impact ejecta carry not only mass but angular momentum as well. Because most ejecta are prograde, they tend to land in the rings at outer distances where the specific angular momentum is larger, so the net resultant drift is inward. Naturally, lower surface density regions are more quickly altered compositionally (e.g., darkened) relative to higher surface density regions.

The value of the micrometeoroid flux at Saturn (now and in the past, when it was most likely greater) still remains uncertain. Past estimates of the micrometeoroid flux at Saturn (Morfill et al. 1983, Ip 1984, Cuzzi & Durisen 1990, Cuzzi & Estrada 1998) vary slightly, but all imply that the main rings would be impacted by close to their own mass over the age of the Solar System (Landgraf et al. 2000). More recently, Galileo measurements at Jupiter have provided estimates of the mass flux accurate to within a factor of two to three (Sremcevic et al. 2005). However, the micrometeorite mass flux at Saturn has not been observed and will not be until the Cassini Extended Mission, which will use an indirect technique similar to that described by Sremcevic et al. (2005). A preliminary estimate from Jones et al. (2008) is within a factor of ten of Cuzzi & Durisen's (1990) estimate.

Meteoroid material darkens and pollutes the rings over time. Doyle et al. (1989), and subsequently Cuzzi & Estrada (1998), noted that the relatively high albedo of the A and B rings is inconsistent with these rings having retained more than a small fraction of primitive, carbonaceous material from the large mass they would have accreted over the age of the Solar System, thereby suggesting a geologically young age for the rings.

3.1.5. Gravitational instability. A gravitational instability occurs when the local self-gravitational potential energy exceeds both the internal energy (due to collisions) and shear kinetic energy (due to Keplerian shear) of the ring particles. Gravitational instability occurs for small values of Toomre's stability criterion Q (Toomre 1964, Karjalainen & Salo 2004), which we define

$$Q = \frac{c\,\Omega}{3.36 G \Sigma}, \tag{8}$$

where c is the local radial velocity dispersion, G is the gravitational constant, Ω is the local Keplerian angular velocity, and Σ is the density. For $Q \lesssim 2$, the collective gravity together with Keplerian shear creates shearing tilted wake structures (by approximately 20° for the Keplerian case) aggregating on timescales comparable with the orbital period (Salo 1995). The typical size of wakes is given by Toomre's critical wavelength (Toomre 1964):

$$\lambda_{\mathrm{crit}} = \frac{4\pi^2 G \Sigma}{\Omega}. \tag{9}$$

Therefore, $\lambda_{\mathrm{crit}} \propto a^{1.5}$ (where a is the distance from Saturn), implying an increase of the wakes' dimensions with distance (assuming $Q \lesssim 2$). For typical values in the A ring, λ_{crit} is 50–100 m, confirmed by stellar occultation data (Section 2.4). Numerical simulations (Salo 1995, Karjalainen & Salo 2004) show that such wakes are progenitors of gravitational aggregates: In the inner regions of the A ring, wakes are like parallel rods with moderate density contrast with the interwave medium, whereas as a increases, the density contrasts increase, and the waves become more clumpy, until a is large enough for these waves to degenerate into individual clumps, recalling small satellites (see **Figure 10**).

3.1.6. Viscous instability and overstability. The first discussion of viscous instability attempted to explain the banded structure of Saturn's B ring seen in Voyager images (Lin & Bodenheimer 1981, Lukkari 1981, Ward 1981, Hämeen-Anttila 1982, Stewart et al. 1984). It is a diffusional instability of sheared collisional systems in which the dependency of the viscosity on surface mass density exhibits a negative derivative for larger density. In that case, the viscous collisional flux is directed away from lower density regions, amplifying any perturbations in the density profile. For dense, flat rings with highly inelastic collisions (as supported by the presence of self-gravity wakes throughout the A and B rings), the viscosity is dominated by nonlocal effects or self-gravity, and this instability does not occur (Schmidt et al. 2009).

Viscous instability: the tendency of a viscous disk to break into a bimodal distribution of low- and high-density regions

Nonetheless, viscous instability could occur for more elastic collisions. In locations where the filling factor is small, local viscosity dominates at small optical depth and nonlocal viscosity is important at large optical depth. In the steady state, the ring breaks into regions of high and low density, with a balance between the dynamically cool, dense regions and the hot, low-density regions. Recently, Salo & Schmidt (2009) proposed the possibility of a size-selective viscous instability.

Viscous overstability is the instability of a ring to inertial acoustic oscillations (Schmidt et al. 2009). If a planetary ring is overstable, it spontaneously develops axisymmetric waves on 100-m scale. These waves are similar to density waves, although they develop without external resonant perturbation. A planetary ring becomes overstable if the viscosity increases steeply enough with optical depth, as expected in dense rings. Axisymmetric 100–200-m wavelike perturbations observed in Saturn's A and B rings are consistent with this process (Colwell et al. 2007, Thomson et al. 2007).

Viscous overstability was proposed by Borderies et al. (1985), and Schmidt & Tscharnuter (1995, 1999) developed a model for Saturn's B ring. Spahn et al. (2000) included the thermal balance equation in this concept. An example of calculations by Salo (2001) is shown in **Figure 19**, which indicates the transition from self-gravity wake domination to overstability. Self-gravity of the ring has a twofold effect on overstable oscillations. On the one hand, self-gravity promotes overstability by steepening the dependency of viscosity on density. On the other hand, in the case of strong self-gravity, the nonaxisymmetric wakes tend to suppress the growth of axisymmetric overstable oscillations, although simulations show that the coexistence of both types of phenomena is permitted. Currently, no analytical theory can model the formation of overstability in a ring with self-gravity wakes (Schmidt et al. 2009).

3.2. Young or Old Rings?

As described by Harris (1984), the rings of the planets likely result from the same process that created the regular satellites. Like the ring particles, the satellite orbits are prograde, equatorial, and nearly circular. A question that immediately arises is whether rings are (*a*) the uncoagulated remnants of satellites that failed to form or (*b*) the result of a disruption of a preexisting object. A related question highlighted by the apparent youth of the rings is whether this latter process of ring creation by satellite destruction continues to the present time. This possibility thus mixes the origin of the rings with their subsequent evolution. Whatever their origin, the sculpted nature of the rings of Saturn, Jupiter, Uranus, and Neptune requires active processes to maintain them.

Because of the short timescale for viscous spreading of the accretion disk of the forming planet, gas drag, particle coagulation, and transport of momentum to the forming planet, Harris (1984) argued that rings did not form contemporaneously with their primary planets but were created later by disruption of satellites whose large size had made them less subject to the early destructive processes. This could be at the end, or well after, the completion of accretion. The pieces of

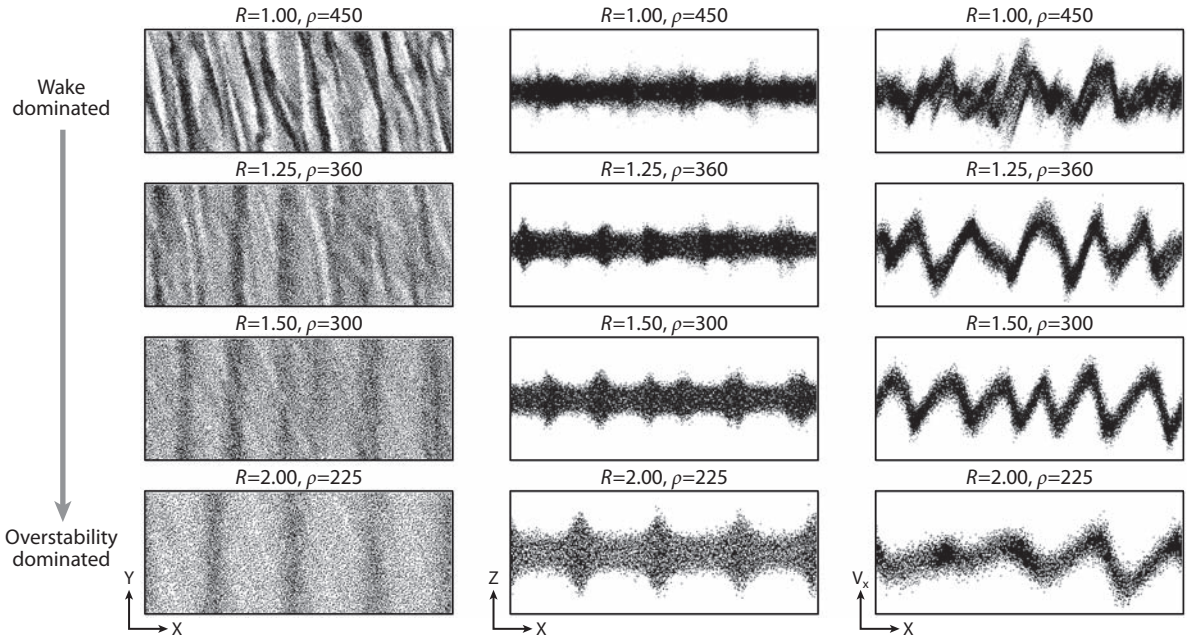

Figure 19

Top and side views of ring regions from numerical simulations showing the transition from wake-dominated (*upper row*) to overstability-dominated ring structures. Figure taken from Salo et al. (2001).

the disrupted satellite are within the Roche zone, where tidal forces keep them from effectively coagulating. This explains naturally the presence of shepherd satellites and ring moons around the various giant planets as the largest pieces remaining after the destruction.

3.2.1. Age of the rings. Spreading of Saturn's A ring due to mutual collisions among the particles (Esposito 1986; see Equation 7) and darkening of the rings due to infall and incorporation of meteoroid material (Doyle et al. 1989, Cuzzi & Estrada 1998) both give ages much younger than the Solar System. Unless confined, the rings spread as their particles exchange momentum via collisions and gravitational scattering (e.g., Goldreich & Tremaine 1982). Even if rings are confined by shepherding satellites, this only slows the spreading process: The momentum is instead transferred to the shepherding moons via the resonance at the ring's edge. Because the moon is more massive than the ring, its evolution is slower, but nonetheless it steadily moves away from the ring due to conservation of angular momentum. If the moon links to yet other moons at resonances, this can further slow the expansion. The abundant density waves in the rings also transfer momentum to the perturbing moons, which likewise recede. For example, tiny Atlas, which orbits just outside Saturn's A ring, would have evolved to its present location in 10–100 million years. Similar short timescales are found for Prometheus and Pandora, the F-ring shepherds. Mutual collisions and meteoroid bombardment grind the ring particles while charged particles sputter molecules from their surfaces.

3.2.2. Collisional cascade. Esposito & Colwell (1989) hypothesized that the nearby moons are the progenitors for future rings. A moon shattered by a large impact from an interplanetary projectile would become a ring of material orbiting the planet. Big moons are the source of small

moons; small moons are the source for rings. Rings are eventually ground to dust that is lost by becoming charged and carried away by the planet's rotating magnetic field or by atmospheric drag into the planetary atmosphere (where it shines briefly as a meteor). They called this process a collisional cascade.

The most serious problem with this explanation is that the collisional cascade uses the raw material (a planet's initial complement of moons) too rapidly. If we imagine we are now looking at the remnants of 4.5 billion years of successive destruction over the age of the Solar System, then this process is almost at its end. The small moons that now remain as the source of future rings have a lifetime of only some few hundred million years, based on calculations by Colwell et al. (2000). This is less than 10% of the age of the Solar System. Why are humans so fortunate as to come upon the scene with robotic space exploration, just in time to see the ring finale?

An alternate explanation is the destruction of a close-passing comet (Dones 1991, Dones et al. 2007). This was the fate of comet Shoemaker-Levy 9 in 1994. As stated by Lissauer et al. (1988) and Ip (1988), such events are rare and unlikely to have occurred in the past billion years. Similar small probabilities can be calculated for the destruction of a moon the size of Mimas in the past billion years. If the rings are even more massive than previously thought (see below), then disruption is even less likely (Robbins et al. 2009). One possible solution is that the ring progenitor (a moon or a comet) could have been destroyed during the Late Heavy Bombardment approximately 700 million years after planet formation. This was a period of great upheaval in the Solar System (Tsiganis et al. 2005). Charnoz et al. (2009b) described how the slow tidal migration in the Saturn system could have left a large moon in the Roche zone until this time, but not for Uranus and Neptune. Thus, Saturn would have had the raw material for its massive ring system. However, this hypothesis would give a ring age of approximately 3.8–3.9 billion years, still much too old to be reconciled with the apparent youth of the rings. In addition, a satellite would likely have a silicate core, no evidence of which is visible in the ring composition.

A possible solution is that the ring material has been recycled. Some evidence for this recycling can be found in Saturn's F ring. Although the F ring is clearly different from the main rings, the same processes of accretion and fragmentation occur there and are more easily visible. If these F-ring processes indicate less obvious ones in Saturn's A and B rings, this can provide a possible explanation of phenomena there. Cassini UVIS star occultations by the F ring detect 39 events ranging from 27 m to 9 km in width (see **Figure 16**). Esposito et al. 2008b interpreted these structures as temporary aggregations of multiple smaller objects, which result from the balance between fragmentation and accretion processes. One of these features was simultaneously observed by VIMS and nicknamed Pywacket. There is evidence that this feature is elongated in azimuth. Some features show sharp edges. At least one F ring object is opaque, nicknamed Mittens, and may be a small moon, not massive enough to clear a gap, and it has been denoted a moonlet. This possible moonlet provides evidence for large objects embedded in Saturn's F ring, which were predicted by Cuzzi & Burns (1988) as the sources of the F ring's material and inferred from Voyager PPS data by Spahn & Wiebicke (1989). F-ring structures and other youthful features detected by Cassini (e.g., see the equatorial bulges in **Figure 20**) may result from ongoing destruction of small parent bodies in the rings and subsequent aggregation of the fragments. If so, the temporary aggregates are at least 10 times more abundant than the solid objects, according to Esposito et al. (2008b).

Recycling of ring material could also explain the limited micrometeoroid darkening of Saturn's rings (Cuzzi & Estrada 1998). Why are the rings not darker now, if they are truly ancient? One possibility is that the total mass of the rings, mostly in Saturn's B ring, has been underestimated. Because the total optical depth of the B ring is still unmeasured and may be more than two times greater than estimated (Colwell et al. 2007, Stewart et al. 2007, Robbins et al. 2009), meteoritic pollution would have a smaller effect. This is seen in the Markov chain simulations of Esposito

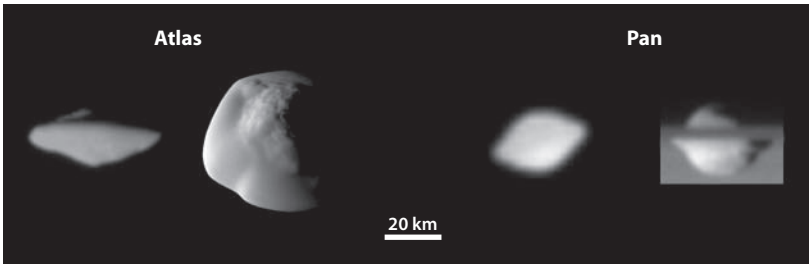

Figure 20

Close-up images of the small moons Atlas and Pan showing equatorial bulges due to accretion. Image courtesy of NASA/JPL/Space Science Institute.

et al. (2008a). If the rings (particularly the B ring) are much more massive than we now estimate, the interior of the largest ring objects (which may encompass most of the ring mass) can remain more pristine until disrupted.

A problem with this proposal is that, in the thinner parts of the rings (where density waves are visible), we have good ring mass estimates that are consistent with the Voyager value. The mass there would be quickly polluted by the meteoroid flux (Cuzzi & Estrada 1998). Esposito (1986) noted that most of the age problems involve Saturn's A ring. Perhaps the A and F rings are more recent? This raises the problem of how the material that formed these possibly more recent rings had been preserved, perhaps as large, unconsolidated objects with competent solid cores encased in rubble? If the A ring is younger, we also need to find an explanation for the Cassini Division. It would not have originated simply by density wave clearing a gap, as proposed by Goldreich & Tremaine (1978).

In conclusion, the rapid evolution of Saturn's rings argues for recent origin, or renewal. Even if recycling is significant, Saturn's A ring and the material in the Cassini Division and the C ring must have been recently emplaced. Most of the ring mass might be in the B ring, where the optical depth is so large we cannot directly measure the mass from density waves. The B ring could have survived longer and be less polluted now, if its mass has been underestimated.

4. CONCLUSIONS AND FUTURE OBSERVATIONS

Saturn's rings appear even more dynamic after the Cassini observations. Instabilities and overstability are evident. Ring particles form temporary aggregations, and the rings are thus clumpy and heterogeneous. The rings are mostly water ice, which is problematic because the rings are continually polluted by micrometeorite impacts. If they were created from the destruction of a small moon or of a comet, they must somehow persist to the present time. Perhaps more massive rings could be recycled?

Many advances in our understanding of the rings were not anticipated prior to Cassini. A key aspect of these advances has been the combination of observations made at different geometries and at different times, as well as the different perspective offered by multiple instruments. We can thus safely anticipate new discoveries from the remainder of Cassini's Equinox Mission and its final extended mission.

Cassini will measure the meteoroid mass flux and the ring mass. During Cassini's Equinox Mission (2008–2010), the spacecraft will fly by Rhea closely to measure the mass flux indirectly, sampling the ejected mass filling its Hill sphere. The geometry of the flyby will make it possible to distinguish this ejecta from whatever equatorial debris might or might not be responsible for

the charged particle absorptions observed by Cassini's fields and particle instruments (Jones et al. 2008). At the end of Cassini's mission, it is hoped that a number of orbits can be implemented with the periapse inward of the D ring. In these close orbits, it is anticipated that a ring mass comparable with Mimas (the post-Voyager consensus; Esposito et al. 1984) can be detected to a few-percent accuracy. A primordial ring compatible with current estimates of meteoritic mass flux would need to be 5–10 times more massive and would be easily detected. Until the time that these fundamental measurements can be made, the question of the ring exposure age to pollution will not be resolved.

As the time baseline of measurements of the dynamic F ring grows longer, we gain a better understanding of the interaction between moon and ring and the growth and destruction of agglomerates within the F-ring region.

The relative spatial precision of Cassini occultation measurements will ultimately enable highly accurate kinematic models of ring features that are linked to moons. The combination of these future developments should shed light on the question of the origin of the rings, as well as how they reached their current configuration.

SUMMARY POINTS

1. Saturn's rings are composed of nearly pure crystalline water ice.
2. Structures in Saturn's rings are radial, azimuthal, and time variable. These are the result of moon perturbations and various instabilities.
3. Moons cause waves and wakes, as well as open gaps (sometimes partially).
4. Rings are unstable to self-gravity wakes, viscous overstability, and possibly viscous instability.
5. Given current observations, investigators cannot yet decide between multiple proposals for the origin of Saturn's rings.
6. Diffuse rings are created by debris from small embedded moons. Saturn's E ring is created by erupted ice grains from Saturn's moon Enceladus.

FUTURE ISSUES

1. Cassini will measure the meteoritic bombardment rate and the total mass of Saturn's rings.
2. Better models can establish the role of fragmentation and accretion in ring history. How do moons and embedded objects affect the outcomes?
3. The combination of observation and theory will determine the origin and evolution of Saturn's rings and allow us to relate our understanding to processes in other planetary ring systems.

DISCLOSURE STATEMENT

The author is not aware of any affiliations, memberships, funding, or financial holdings that might be perceived as affecting the objectivity of this review.

ACKNOWLEDGMENTS

I appreciate helpful comments from Mark Lewis, Glen Stewart, Matt Tiscareno, Miodrag Sremcevic, Nicole Albers, and Juergen Schmidt. This work was supported by the Cassini Project.

LITERATURE CITED

Albers N, Spahn F. 2006. The influence of particle adhesion on the stability of agglomerates in Saturn's rings. *Icarus* 181:292–301

Albers N, Sremcevic M, Colwell JE, Esposito LW. 2010. Saturn's F ring as seen by Cassini UVIS: kinematics and statistics. *Icarus*. In press

Barbara JM, Esposito LW. 2002. Moonlet collisions and the effects of tidally modified accretion in Saturn's F ring. *Icarus* 160:161–71

Borderies N, Goldreich P, Tremaine S. 1985. A granular flow model for dense planetary rings. *Icarus* 63:406–20

Brahic A. 1976. Numerical simulation of a system of colliding bodies in a gravitational field. *J. Comput. Phys.* 22:171–88

Burns JA, Tiscareno MS, Spitale J, Porco CC, Cooper NJ, et al. 2008. Giant propellers outside the Encke gap in Saturn's rings. *AAS/Div. Planet. Sci. Meet. Abstr.* 40:30.07

Camichel H. 1958. Mesures photométriques de Saturne et de son anneau. *Ann. Astrophys.* 21:231–42

Canup RM, Esposito LW. 1995. Accretion in the Roche zone: coexistence of rings and ring moons. *Icarus* 113:331–52

Chakrabarti SK. 1989. The dynamics of particles in the bending waves of planetary rings. *MNRAS* 238:1381–94

Chandrasekhar S. 1969. *Ellipsoidal Figures of Equilibrium*. The Silliman Found. Lect. New Haven, CT: Yale Univ. Press

Charnoz S. 2009. Physical collisions of moonlets and clumps with the Saturn's F-ring core. *Icarus* 201:191–97

Charnoz S, Dones L, Esposito LW, Estrada PR, Hedman MM. 2009a. Origin and evolution of Saturn's ring system. See Dougherty et al. 2009, pp. 537–75

Charnoz S, Morbidelli A, Dones L, Salmon J. 2009b. Did Saturn's rings form during the Late Heavy Bombardment? *Icarus* 199:413–28

Charnoz S, Porco CC, Déau E, Brahic A, Spitale JN, et al. 2005. Cassini discovers a kinematic spiral ring around Saturn. *Science* 310:1300–4

Colwell JE, Cooney JH, Esposito LW, Sremcevic M. 2009a. Density waves in Cassini UVIS stellar occultations: 1. The Cassini Division. *Icarus* 200(2):574–80

Colwell JE, Esposito LW, Bundy D. 2000. Fragmentation rates of small satellites in the outer solar system. *J. Geophys. Res.* 105:17589–600

Colwell JE, Esposito LW, Sremcevic M. 2006. Self-gravity wakes in Saturn's A ring measured by stellar occultations from Cassini. *Geophys. Res. Lett.* 33:L07201

Colwell JE, Esposito LW, Sremcevic M, Stewart GR, McClintock WE. 2007. Self-gravity wakes and radial structure of Saturn's B ring. *Icarus* 190:127–44

Colwell JE, Nicholson PD, Tiscareno MS, Murray CD, French RG, Marouf EA. 2009b. The structure of Saturn's rings. See Dougherty et al. 2009, pp. 375–412

Cook AF, Franklin FA. 1964. Rediscussion of Maxwell's Adams Prize Essay on the stability of Saturn's rings. *Astron. J.* 69:173–200

Cuzzi JN, Burns JA. 1988. Charged particle depletion surrounding Saturn's F ring: evidence for a moonlet belt? *Icarus* 74:284–324

Cuzzi J, Clark R, Filacchione G, French R, Johnson R, et al. 2009. Ring particle composition and size distribution. See Dougherty et al. 2009, pp. 459–509

Cuzzi JN, Colwell JE, Esposito LW, Porco CC, Murray CE, et al. 2004. Saturn's rings: pre-Cassini status and mission goals. *Space Sci. Rev.* 104:209–51

Cuzzi JN, Durisen RH. 1990. Meteoroid bombardment of planetary rings: general formulation and effects of Oort cloud projectiles. *Icarus* 84:467–501

Cuzzi JN, Estrada PR. 1998. Compositional evolution of Saturn's rings due to meteoroid bombardment. *Icarus* 132:1–35

Cuzzi JN, Lissauer JJ, Esposito LW, Holberg JB, Marouf EA, et al. 1984. Saturn's rings: properties and processes. See Greenberg & Brahic 1984, pp. 73–199
Daisaka H, Tanaka H, Ida S. 2001. Viscosity in a dense planetary ring with self-gravitating particles. *Icarus* 154:296–312
Dones L. 1991. A recent cometary origin for Saturn's rings? *Icarus* 92:194–203
Dones L, Agnor CB, Asphaug E. 2007. Formation of Saturn's rings by tidal disruption of a Centaur. *Bull. Am. Astron. Soc.* 38:420
Dougherty M, Esposito L, Krimigis T, eds. 2009. *Saturn from Cassini-Huygens*. Heidelberg: Springer
Doyle LR, Dones L, Cuzzi JN. 1989. Radiative transfer modeling of Saturn's outer B ring. *Icarus* 80:104–35
Durisen RH. 1984a. Particle erosion mechanisms and mass redistribution in Saturn's rings. *Adv. Space Res.* 4:13–21
Durisen RH. 1984b. Transport effects due to particle erosion mechanisms. See Greenberg & Brahic 1984, pp. 416–46
Esposito LW. 1986. Structure and evolution of Saturn's rings. *Icarus* 67:345–57
Esposito LW. 1993. Understanding planetary rings. *Annu. Rev. Earth Planet. Sci.* 21:487–523
Esposito LW. 2002. Planetary rings. *Rep. Prog. Phys.* 65:1741–83
Esposito LW. 2006. *Planetary Rings*. Cambridge, UK: Cambridge Univ. Press
Esposito LW, Colwell JE. 1989. Creation of the Uranus rings and dust bands. *Nature* 339:605–7
Esposito LW, Colwell JE, Larsen K, McClintock WE, Stewart AIF, et al. 2005. Ultraviolet imaging spectroscopy shows an active Saturnian system. *Science* 307:1251–55
Esposito LW, Cuzzi JN, Holberg JB, Marouf EA, Tyler GL, et al. 1984. Saturn's rings: structure, dynamics, and particle properties. See Greenberg & Brahic 1984, pp. 463–545
Esposito LW, Elliott JP, Albers N. 2008a. Regolith growth and darkening of Saturn's ring particles. *Am. Geophys. Union Meet. 2008* Abstr. No. P13A-1295
Esposito LW, Meinke BK, Colwell JE, Nicholson PD, Hedman MH. 2008b. Moonlets and clumps in Saturn's F ring. *Icarus* 194:278–89
Esposito LW, O'Callaghan M, West RA. 1983. The structure of Saturn's rings: implications from the Voyager stellar occultation. *Icarus* 56:439–52
French RG, McGhee CA, Dones L, Lissauer JJ. 2003. Saturn's wayward shepherds: the peregrinations of Prometheus and Pandora. *Icarus* 162:143–70
French RG, Salo H, McGhee CA, Dones L. 2007. HST observations of azimuthal asymmetry in Saturn's rings. *Icarus* 189(2):493–522
Gehrels T, Baker LR, Beshore E, Blenman C, Burke JJ, et al. 1980. Imaging photopolarimeter on Pioneer Saturn. *Science* 207:434–39
Goldreich P, Rappaport N. 2003. Chaotic motions of Prometheus and Pandora. *Icarus* 162:391–99
Goldreich P, Tremaine SD. 1978. The velocity dispersion in Saturn's rings. *Icarus* 34:227–39
Goldreich P, Tremaine SD. 1979. Toward a theory of the Uranian rings. *Nature* 277:97–99
Goldreich P, Tremaine SD. 1982. Dynamics of planetary rings. *Annu. Rev. Astron. Astrophys.* 20:249–83
Greenberg R, Brahic A, eds. 1984. *Planetary Rings*. Tucson: Univ. Ariz. Press
Hämeen-Anttila KA. 1982. Saturn's rings and bimodality of Keplerian systems. *Earth Moon Planets* 26:171–96
Harris A. 1984. The origin and evolution of planetary rings. See Greenberg & Brahic 1984, pp. 641–59
Hedman MM, Burns JA, Tiscareno MS, Porco CC, Jones G, et al. 2007a. The source of Saturn's G ring. *Science* 317:653–56
Hedman MM, Murray CD, Cooper NJ, Tiscareno MS, Beurle K, et al. 2009. Three tenuous rings/arcs for three tiny moons. *Icarus* 199:378–86
Hedman MM, Nicholson PD, Salo H, Wallis BD, Buratti BJ, et al. 2007b. Self-gravity wake structures in Saturn's A ring revealed by Cassini VIMS. *Astron. J.* 133:2624–29
Horanyi M, Burns JA, Hedman MM, Jones GH, Kempf S. 2009. Diffuse rings. See Dougherty et al. 2009, pp. 511–36
Ip W-H. 1983. Collisional interactions of ring particles: the ballistic transport process. *Icarus* 54:253–62
Ip W-H. 1984. Ring torque of Saturn from interplanetary meteoroid impact. *Icarus* 60:547–52
Ip W-H. 1988. An evaluation of a catastrophic fragmentation origin of the Saturnian ring system. *Astron. Astrophys.* 199:340–42

Johnson RE, Luhmann JG, Tokar RL, Bouhram M, Berthelier JJ, et al. 2006. Production, ionization and redistribution of O_2 Saturn's ring atmosphere. *Icarus* 180:393–402
Jones GH, Roussos E, Krupp N, Beckmann U, Coates AJ, et al. 2008. The dust halo of Saturn's largest icy moon Rhea. *Science* 319:1380–84
Julian WH, Toomre A. 1966. Non-axisymmetric responses of differentially rotating disks of stars. *Astrophys. J.* 146:810–27
Karjalainen R, Salo H. 2004. Gravitational accretion of particles in Saturn's rings. *Icarus* 172:328–48
Kempf S, Beckmann U, Schmidt J. 2009. How the Enceladus dust plume feeds Saturn's E ring. *Icarus*. In press, doi:10.1016/j.icarus.2009.09.016
Lagage PO, Pantin E. 1994. Dust depletion in the inner disk of Beta-Pictoris as a possible indicator of planets. *Nature* 369:628–30
Landgraf M, Baggaley WJ, Grün E, Krüger H, Linkert G. 2000. Aspects of the mass distribution of interstellar dust grains in the Solar System from in-situ measurements. *J. Geophys. Res.* 105:10343–52
Lewis MC, Stewart GR. 2005. Expectations for Cassini observations of ring material with nearby moons. *Icarus* 178:124–43
Lewis MC, Stewart GR. 2009. Features around embedded moonlets in Saturn's rings: the role of self-gravity and particle size distributions. *Icarus* 199:387–412
Leyrat C, Spilker LJ, Altobelli N, Pilorz S, Ferrari C. 2008. Infrared observations of Saturn's rings by Cassini CIRS: phase angle and local time dependence. *Planet Space Sci.* 56:117–33
Lin DNC, Bodenheimer P. 1981. On the stability of Saturn' rings. *Astrophys. J. Lett.* 248:L83–86
Lissauer JJ. 1984. Ballistic transport in Saturn's rings: an analytical theory. *Icarus* 57:63–71
Lissauer JJ. 1985. Bending waves and the structure of Saturn's rings. *Icarus* 62:433–47
Lissauer JJ, Shu FH, Cuzzi JN. 1984. Viscosity in Saturn's rings. In *Planetary Rings, Proc. IAU Symp. No. 75*, ed. A Brahic, pp. 385–92. Toulouse, France
Lissauer JJ, Squyres SW, Hartmann WK. 1988. Bombardment history of the Saturn system. *J. Geophys. Res.* 93:13776–804
Lukkari J. 1981. Collisional amplification of density fluctuations in Saturn's rings. *Nature* 292:433–35
Lumme K, Irvine WM, Esposito LW. 1983. Theoretical interpretation of the ground-based photometry of Saturn's B ring. *Icarus* 53:174–84
Lynden-Bell D, Pringle FE. 1974. The evolution of viscous discs and the origin of the nebular variables. *MNRAS* 168:603–37
Masset FS, Papaloizou JCB. 2003. Runaway migration and the formation of hot Jupiters. *Astrophys. J.* 588:494–508
Morfill GE, Fechtig H, Grün E, Goertz C. 1983. Some consequences of meteoroid bombardment of Saturn's rings. *Icarus* 55:439–47
Murray CD, Beurle K, Cooper NJ, Evans MW, Williams GA, et al. 2008. The determination of the structure of Saturn's F ring by nearby moonlets. *Nature* 453:739–44
Murray CD, Chavez C, Beurle K, Cooper N, Evans MW, et al. 2005. How Prometheus creates structure in Saturn's F ring. *Nature* 437:1326–29
Nicholson PD, Cooke ML, Pelton E. 1990. An absolute radius scale for Saturn's rings. *Astron. J.* 100:1339–62
Papaloizou JCB, Nelson RP, Kley W, Masset FS, Artymowicz P. 2007. Disk-planet interactions during planet formation. In *Protostars and Planets V*, ed. B Reipurth, D Jewitt, K Keil, pp. 655–68. Tucson: Univ. Ariz. Press
Porco CC, Baker E, Barbara J, Beurle K, Brahic A, et al. 2005. Cassini imaging science: initial results on Saturn's rings and small satellites. *Science* 307:1226–36
Porco C, Weiss J, Richardson D, Dones L, Quinn T, et al. 2008. Simulations of the dynamical and light-scattering behavior of Saturn's rings and the derivation of ring particle and disk properties. *Astron. J.* 136:2172–200
Poulet F, Sicardy B, Nicholson PD, Karkoschka E, Caldwell J. 2000. Saturn's ring-plane crossings of August and November 1995: a model for the new F-ring objects. *Icarus* 144:135–48
Robbins SJ, Stewart GR, Lewis MC, Colwell JE, Sremcevic M. 2009. Estimating the masses of Saturn's A and B rings from high-optical depth *N*-body simulations and stellar occultations. *Icarus*. In press, doi:10.1016/j.icarus.2009.09.012

Roche EA. 1847. Académie des sciences et lettres de Montpellier. *Mém. Sect. Sci.* 1:243–62
Rosen PA, Tyler GL, Marouf EA, Lissauer JJ. 1991. Resonance structures in Saturn's rings probed by radio occultation. II. Results and interpretation. *Icarus* 93:25–44
Salo H. 1992. Gravitational wakes in Saturn's rings. *Nature* 359:619–21
Salo H. 1995. Simulations of dense planetary rings. III. Self-gravitating identical particles. *Icarus* 117:287–312
Salo H. 2001. Numerical simulations of the collisional dynamics of planetary rings. In *Granular Gases*, ed. T Pöschel, S Luding, pp. 330–49. Lect. Notes Phys. Vol. 564. Berlin: Springer Verlag
Salo H, Karjalainen R. 2003. Photometric modeling of Saturn's rings. I. Monte Carlo method and the effect of nonzero volume filling factor. *Icarus* 164:428–60
Salo H, Schmidt J. 2009. N-body simulations of viscous instability of planetary rings. *Icarus*. In press, doi:10.1016/j.icarus.2009.07.038
Salo H, Schmidt J, Spahn F. 2001. Viscous overstability in Saturn's B ring. I. Direct simulations and measurement of transport coefficients. *Icarus* 153:295–315
Schmidt J, Ohtsuki K, Rappaport N, Salo H, Spahn F. 2009. Dynamics of Saturn's dense rings. See Dougherty et al. 2009, pp. 413–58
Schmit U, Tscharnuter W. 1995. A fluid dynamical treatment of the common action of self-gravitation, collisions, and rotation in Saturn's B-ring. *Icarus* 115:304–19
Schmit U, Tscharnuter W. 1999. On the formation of the fine-scale structure in Saturn's B ring. *Icarus* 138:173–87
Showalter MR. 1991. Visual detection of 1981S 13, Saturn's eighteenth satellite, and its role in the Encke gap. *Nature* 351:709–13
Showalter MR. 1998. Detection of centimeter-sized meteoroid impact events in Saturn's F ring. *Science* 282:1099–102
Showalter MR. 2004. Disentangling Saturn's F ring. I. Clump orbits and lifetimes. *Icarus* 171:356–71
Showalter MR, Pollack JB, Ockert ME, Doyle LR, Dalton JB. 1992. A photometric study of Saturn's F ring. *Icarus* 100:394–411
Shu FH, Dones L, Lissauer JJ, Yuan C, Cuzzi JN. 1985. Nonlinear spiral density waves: viscous damping. *Astrophys. J.* 299:542–73
Smith BA, Soderblom L, Batson R, Bridges P, Inge J, et al. 1982. A new look at the Saturn system: the Voyager 2 images. *Science* 215(4532):504–37
Smith BA, Soderblom L, Beebe R, Boyce J, Briggs G, et al. 1981. Encounter with Saturn: Voyager 1 imaging science results. *Science* 212:163–91
Smoluchowski R. 1978. Width of a planetary ring system and the C-ring of Saturn. *Nature* 274:669–70
Smoluchowski R. 1979. The ring systems of Jupiter, Saturn and Uranus. *Nature* 280:377–78
Spahn F, Schmidt J, Petzschmann O, Salo H. 2000. Stability analyses of a Keplerian disk of granular grains: influence of thermal diffusion. *Icarus* 145:657–60
Spahn F, Sremcevic M. 2000. Density patterns induced by small moonlets in Saturn's rings? *Astron. Astrophys.* 358:368–72
Spahn F, Wiebicke H-J. 1989. Long-term gravitational influence of moonlets in planetary rings. *Icarus* 77:124–34
Spilker LJ, Pilorz S, Lane AL, Nelson RM, Pollard B, Russell CT. 2004. Saturn A ring surface mass densities from spiral density wave dispersion behavior. *Icarus* 171:372–90
Sremcevic M, Krivov AV, Krüger H, Spahn F. 2005. Impact-generated dust clouds around planetary satellites: model versus Galileo data. *Planet. Space Sci.* 53:625–41
Sremcevic M, Schmidt J, Salo H, Seiß M, Spahn F, et al. 2007. A belt of moonlets in Saturn's A ring. *Nature* 449:1019–21
Stewart GR, Lin DNC, Bodenheimer P. 1984. Collision-induced transport processes in planetary rings. See Greenberg & Brahic 1984, pp. 447–512
Stewart GR, Robbins SJ, Colwell JE. 2007. Evidence for a primordial origin of Saturn's rings. *39th Div. Planet. Sci. Meet.* Abstract. No. 7.06
Thomson F, Marouf EA, Tyler GL, French RG, Rappaport NJ. 2007. Periodic microstructure in Saturn's rings A and B. *Geophys. Res. Lett.* 34:L24203

Tiscareno MS, Burns JA, Hedman MM, Porco CC. 2008. The population of propellers in Saturn's A ring. *Astron. J.* 135:1083–91

Tiscareno MS, Burns JA, Hedman MM, Porco CC, Weiss JW, et al. 2006a. 100-metre-diameter moonlets in Saturn's A ring from observations of 'propeller' structures. *Nature* 440:648–50

Tiscareno MS, Burns JA, Nicholson PD, Hedman MM, Porco CC. 2007. Cassini imaging of Saturn's rings. II. A wavelet technique for analysis of density waves and other radial structure in the rings. *Icarus* 189:14–34

Tiscareno MS, Nicholson PD, Burns JA, Hedman MM, Porco CC. 2006b. Unravelling temporal variability in Saturn's spiral density waves: results and predictions. *Astrophys. J.* 651:L65–68

Toomre A. 1964. On the gravitational stability of a disk of stars. *Astrophys. J.* 139:1217–38

Tsiganis K, Gomes R, Morbidelli A, Levison HF. 2005. Origin of the orbital architecture of the giant planets of the solar system. *Nature* 435:459–61

Ward WR. 1981. On the radial structure of Saturn's rings. *Geophys. Res. Lett.* 8:641–43

Weidenschilling SJ, Chapman CR, Davis DR, Greenberg R. 1984. Ring particles. See Greenberg & Brahic 1984, pp. 367–415

Annual Review
of Earth and
Planetary Sciences

Volume 38, 2010

Contents

Indexes

Errata

An online log of corrections to *Annual Review of Earth and Planetary Sciences* articles may be found at http://earth.annualreviews.org